Calcium Isotopic Evidence for Vulnerable Marine Ecosystem Structure Prior to the K/Pg Extinction

Jérémy Martin, Peggy Vincent, Theo Tacail, Fatima Khaldoune, Essaid Jourani, Nathalie Bardet, Vincent Balter

Calcium isotopic evidence for vulnerable marine ecosystem structure prior to the K-Pg extinction

Jeremy E. Martin[1, 2*], Peggy Vincent[3], Théo Tacail[1], Fatima Khaldoune[4], Essaid Jourani[4], Nathalie Bardet[3], and Vincent Balter[1]

[1]Université Lyon, ENS de Lyon, Université Lyon 1, CNRS, UMR 5276 Laboratoire de Géologie de Lyon: Terre, Planète, Environnement, F-69342 Lyon, France

[2]Lead Contact

[3]Sorbonne Universités – CR2P – MNHN, CNRS, UPMC-Paris 6, Muséum national d'Histoire naturelle, 57 rue Cuvier, CP 38, 75231 Paris cedex 05, France

[4]Direction de la géologie, OCP SA, Morocco

*Correspondance : jeremy.martin@ens-lyon.fr

SUMMARY

The collapse of marine ecosystems during the end-Cretaceous mass extinction involved the base of the foodchain [1] up to ubiquitous vertebrate apex predators [2–5]. Large marine reptiles became suddenly extinct at the Cretaceous-Paleogene (K-Pg) boundary whereas other contemporaneous groups such as bothremydid turtles or dyrosaurid crocodylomorphs, although affected at the familial, genus or species level, survived into post-crisis environments of the Paleocene [5–9] and could have found refuge in freshwater habitats [11–13]. A recent hypothesis proposes that the extinction of plesiosaurians and mosasaurids could have been caused by an important drop in sea level [10]. Mosasaurids are unusually diverse and locally abundant in the

Maastrichtian phosphatic deposits of Morocco, and with large sharks and one species of elasmosaurid plesiosaurian recognized so far, contribute to an overabundance of apex predators [3, 7, 14, 15]. For this reason, high local diversity of marine reptiles exhibiting different body masses and a wealth of tooth morphologies hints at complex trophic interactions within this latest Cretaceous marine ecosystem. Using calcium isotopes, we investigate the trophic structure of this extinct assemblage. Our results are consistent with a calcium isotope pattern observed in modern marine ecosystems and show that plesiosaurians and mosasaurids indiscriminately fall in the tertiary piscivore group. This suggests that marine reptile apex predators relied onto a single dietary calcium source, compatible with the vulnerable wasp-waist food webs of the modern world [16]. This inferred peculiar ecosystem structure may help explain plesiosaurian and mosasaurid extinction following the end-Cretaceous biological crisis.

KEYWORDS

Calcium isotopes, Paleoecology, Marine ecosystem, Cretaceous, Mass extinction, Wasp-waist food web, Marine reptiles

RESULTS AND DISCUSSION

Following recent studies on modern marine vertebrates [17–20], we use calcium isotopes to assess trophic relationships among the diverse vertebrates that inhabit the Late Maastrichtian marine ecosystem of the Moroccan phosphatic basin. Calcium is a readily available and soluble element in seawater, amounting to about 420 p.p.m. [21]. As a major element of bioapatite, it amounts to about 40% of tooth enamel, the most compact biological material. As measured in seawater, invertebrates and vertebrates, a trophic level effect is observed showing decreasing

calcium isotope values (expressed below as $\delta^{44/42}Ca$) with increasing trophic position [17–20]. Therefore, in the marine environment, the calcium isotope composition of mineralized biological tissues such as bone or teeth can be interpreted in terms of trophic inference. Case studies on marine fossil vertebrates have been restricted to Neogene assemblages and recover a similar trophic level effect as in the modern world [19–20]. Given the high crystallinity of bioapatite in enamel and its high preservation potential, this method is applied here to older material [22, 23].

In this study, marine vertebrates, comprising 16 species from a single level (C2) in the Benguerir section of the Ganntour basin, Morocco (see [14] for stratigraphical details), were analyzed for calcium isotopes (see STAR Methods and Table S1). Importantly, the range of calcium isotope values measured in the Cretaceous vertebrate assemblage from Benguerir section mirrors the trophic levels recovered in modern marine ecosystems [20]. This provides a robust case against a complete diagenetic overprinting of the biogenic isotope calcium composition. Results show identical calcium isotope values with or without pretreatment (Fig. S2)

In the studied fossil assemblage (Fig. 1), the least fractionated $\delta^{44/42}Ca$ value is represented by the marine turtle group (– 0.40 ± 0.04 ‰ 1SD, n = 5) and shows a $\Delta^{44/42}Ca$ relative to Late Maastrichtian seawater of - 0.70 ‰, which is identical to the $\Delta^{44/42}$ between modern turtles and modern seawater. A second fossil group includes pycnodonts and teleost fishes with the barracuda-like *Enchodus* as well as two sawsharks of the genus *Pristiphorus* and has an intermediate mean value (– 0.57 ± 0.12 1SD, n = 8) and a $\Delta^{44/42}Ca$ relative to Late Maastrichtian seawater of - 0.87‰, which is indistinguishable from the $\Delta^{44/42}Ca$ value observed between the modern primary piscivore group and modern seawater (- 0.87‰). The group containing the large sharks *Cretolamna*, *Squalicorax* and *Carcharias* (– 0.86 ± 0.17‰ 1SD, n =

7) has a $\Delta^{44/42}$Ca relative to Late Maastrichtian seawater of - 1.16‰ and is thus very close to the $\Delta^{44/42}$Ca between modern tertiary piscivores and modern seawater (- 1.13‰). Marine reptiles calcium isotope values strongly overlap with the large sharks but display slightly lower values in average (– 0.93 ± 0.12 % 1SD, n = 31). Values for the elasmosaurid plesiosaurian and the five mosasaurid genera are indistinguishable, suggesting that they indiscriminately fed on the same calcium source.

The relatively homogenous calcium isotope values measured in marine reptile enamel imply that the calcium source, i.e. preys, irrespective of their nature, had a comparable calcium isotope composition. Considering a systematic $\Delta^{44/42}$Ca shift of about - 0.14 ‰ from diet to consumer [20], our results point to a common calcium source for the diet of the large sharks and predatory marine reptiles. A single outlier is represented by a specimen of *Globidens* (out of seven), which presents a relatively enriched calcium isotope composition relative to other marine reptiles, indicating a heavy calcium-rich food source at least for some individuals.

The calcium isotope data do not allow us to recognize any resource partitioning among predatory marine reptiles. Such results may instead reflect a single dietary source, or at least different dietary sources of identical trophic levels, which contrasts markedly with previous studies that documented an impressive diversity of trophic guilds based on mosasaurid tooth morphologies [7, 24]. For example, the massive bulbous dentition of *Globidens* has been hypothesized to serve a crushing function whereas conical/blade-like teeth of other mosasaurid species and of elasmosaurid plesiosaurians could serve puncturing or cutting functions [7]. This apparent discrepancy might be explained by the peculiar ecosystem structure of the Maastrichtian phosphatic deposits of Morocco.

Here, the structure of the Late Maastrichtian marine ecosystem, as inferred from calcium isotopes, differs in its composition from modern assemblages where apex predators are represented by birds and mammals but also by selachians. By contrast, our data point to a single dietary source for apex predators, suggesting a bottom-up control, with a considerable biomass sustaining an abundant and diversified assemblage of large apex predators. A comparable structure, known as wasp-waisted, is observed in modern upwelling environments, where a large biomass of poorly diversified forage organisms (the intermediate trophic level) exerts a bottom-up control on diverse apex predators and exerts a top-down control on invertebrate preys [16, 25]. This inference is in perfect agreement with the sedimentological data from the study sites [26], which indicate that the studied fossiliferous phosphate strata were deposited under an upwelling environment. We therefore interpret our results as providing strong evidence for as a wasp-waist structure in the studied Late Maastrichtian assemblage. As a caveat, it should be stressed out that the structure of modern upwelling ecosystems has not yet been investigated using calcium isotopes.

Our results have implications for the extinction of marine reptiles at the K/Pg boundary. The latest Cretaceous was marked by a major expansion of phosphate deposits in the intertropical zone, interpreted to reflect intensified upwellings related to the opening of the Atlantic Ocean [26]. In parallel, plesiosaurians and mosasaurids became particularly widespread, diversified and abundant. Although the wasp-waist structure evidenced by our data for the Moroccan upwelling ecosystem deserves further testing in coeval marine assemblages, it can be reasonably hypothesized that a similar structure characterized many, if not all of these low-latitude upwelling ecosystems. If correct, this widespread wasp-waist structure may have rendered latest Cretaceous ecosystems particularly vulnerable to environmental perturbations of

the K/Pg. As a modern example, the drop in abundance and diversity of apex predators in modern upwelling environments is a result of sardine and anchovy overexploitation by industrial fisheries of the late XIXth century [16]. Accordingly, the collapse of phytoplankton at the K/Pg boundary [1, 27], likely had a severe impact on intermediate and higher trophic levels occupied by selachians and marine reptiles [6]. This collapse would have been particularly detrimental to plesiosaurians and mosasaurids, which possessed a higher metabolic rate than crocodylomorphs or selachians [28], necessitating substantial caloric intake, hence a corresponding biomass available as prey. This may have been especially sustainable in upwelling zones, which are highly productive environments but are extremely vulnerable ecosystems in contrast to reef ecosystems [29]. The sudden environmental catastrophe disrupting primary productivity at the K/Pg boundary combined with a widespread and vulnerable type of ecosystem likely had drastic effects across apex predator communities. Together with models inferring biotic interactions in Cretaceous terrestrial ecosystems [30], our results highlight that the collapse of Maastrichtian marine ecosystems was timely and could have been partly explained by their vulnerable nature characterized by a wasp-waist structure.

AUTHOR CONTRIBUTIONS

The project was conceived by J.E.M., P.V., T.T., N.B. and V.B. Specimens were retrieved in the field by P.V., N.B., F.K. and E.J.. J.E.M. and P.V. sampled the specimens and conducted purification in the clean lab. J.E.M. and T.T. performed MC-ICP-MS measurements. All authors discussed the results. The first draft version of the text was written by J.E.M. then subsequently, P.V., T.T., N.B., V.B., F.K. and E.J. contributed to it.

ACKNOWLEDGMENTS

This work was performed under the convention “Cadre Phosphapal” of the cooperation between OCP, Ministère de l’Energie, des Mines, de l’Eau et de l’Environnement du Royaume du Maroc, Université Cadi Ayyad, Marrakech, Morocco and MHNH, France. We thank E. Robert (UMR CNRS 5276, LGLTPE) for allowing us to sample modern turtle bone curated in the collections of Université Claude Bernard Lyon 1. For technical assistance on spectrometers, we thank E. Albalat, F. Arnaud-Gousset and P. Telouk.

REFERENCES

1. Smit, J., and Hertogen, J. (1980). An extraterrestrial event at the Cretaceous-Tertiary boundary. Nature *285*, 198–200.
2. Russell, D.A. (1967). Systematics and morphology of American mosasaurs. Bull. Peabody Mus. Nat. Hist. *23*, 1–241.
3. Bardet, N., Pereda Suberbiola, X., Jouve, S., Bourdon, E., Vincent, P., Houssaye, A., Rage, J.-C., Jalil, N.-E., Bouya, B., and Amaghzaz, M. (2010). Reptilian assemblages from the latest Cretaceous–Palaeogene phosphates of Morocco: from Arambourg to present time. Hist. Biol. *22*, 186–199.
4. Bardet, N., Falconnet, J., Fischer, V. Houssaye, A., Jouve, S., Pereda Suberbiola, X., Perez-Garcia, A., Rage, J.-C., and Vincent, P. (2014). Mesozoic marine palaeobiogeography in response to drifting plate. Gond. Res. *26*, 869–887.
5. Vincent, P., Bardet, N., Pereda Suberbiola, X., Bouya, B., Amaghzaz, M., and Meslouh, S. (2011). *Zarafasaura oceanis*, a new elasmosaurid (Reptilia: Sauropterygia) from the

Maastrichtian Phosphates of Morocco and the palaeobiogeography of latest Cretaceous plesiosaurs. Gond. Res. *19*, 1062–1073.

6. Bardet, N. (1994). Extinction events among Mesozoic marine reptiles. Hist. Biol. *7*, 313-324.

7. Bardet, N., Houssaye, A., Vincent, P., Pereda Suberbiola, X., Amaghzaz, M., Jourani, E., and Meslouh, S. (2015). Mosasaurids (Squamata) from the Maastrichtian Phosphates of Morocco: biodiversity, palaeobiogeography and palaeoecology based on tooth morphoguilds. Gond. Res. *27*, 1068–1078.

8. Jouve, S., Bardet, N., Jalil, N., Pereda-Suberbiola, X., Bouya, B., and Amaghzaz, M. (2008). The oldest African crocodile: phylogeny, paleobiogeography, and differential survivorship of marine reptile through the Cretaceous-Tertiary boundary. J. Vertebr. Paleontol. *28*, 409–421.

9. Martin, J. E., Amiot, R., Lécuyer, C., and Benton, M. J. (2014). Sea surface temperature contributes to marine crocodylomorph evolution. Nat. comm. doi: 10.1038/ncomms5658B.

10. Benson, R. B. J., and Butler, R. J. (2011). Uncovering the diversification history of marine tetrapods: ecology influences the effect of geological sampling biases. Spec. Pub. Geol. Soc. Lond. *358*, 191–208.

11. Buffetaut, E. (1984). Selective extinctions and terminal Cretaceous events Nature *310*, 276.

12. Buffetaut, E. (1990). Vertebrate extinctions and survival across the Cretaceous–Tertiary boundary. Tectonophysics *171*, 337–345.

13. Hill, R. V., McCartney, J. A., Roberts, E., Bouaré, M., Sissoko, F., and O'Leary, M. (2008). Dyrosaurid (Crocodyliformes: Mesoeucrocodylia) fossils from the Upper Cretaceous and Paleogene of Mali: implications for phylogeny and survivorship across the K/T boundary. Am. Mus. Nov. *3631*, 1–19.

14. Cappetta, H., Bardet, N., Pereda Suberbiola, X., Adnet, S., Akkrim, D., Amalik, M., and Benabdallah, A. (2014). Marine vertebrate faunas from the Maastrichtian phosphates of Benguérir (Ganntour Basin, Morocco): biostratigraphy, palaeobiogeography and palaeoecology. Palaeogeogr., Palaeoclim., Palaeoecol. *409*, 217–238.

15. Vincent, P., Bardet, N., Houssaye, A., Amaghzaz, M., and Meslouh, S. (2013). New plesiosaur specimens from the Maastrichtian Phosphates of Morocco and their implications for the ecology of the latest Cretaceous marine apex predators. Gond. Res. *24*, 796–805.

16. Cury, P., Bakun, A., Crawford, R.J.M., Jarre, A., Quiñones, R.A., Shannon, L.J., and Verheye, H.M. (2000). Small pelagics in upwelling systems: patterns of interaction and structural changes in "wasp-waist" ecosystems. ICES J. Mar. Sci. *57*, 603–618.

17. Skulan, J., DePaolo, D.J., and Owens, T.L. (1997). Biological control of calcium isotopic abundances in the global calcium cycle. Geoch. Cosm. Acta *61*, 2505–2510.

18. Skulan, J., and DePaolo, D.J. (1999). Calcium isotope fractionation between soft and mineralized tissues as a monitor of calcium use in vertebrates. Proc. Nat. Acad. Sci. U.S.A. *96*, 13709–13713.

19. Clementz, M.T., Holden, P., and Koch, P.L. (2003). Are calcium isotopes a reliable monitor of trophic level in marine settings? Inter. J. Osteoarchaeol. *13*, 29–36.

20. Martin, J.E., Tacail, T., Adnet, S., Girard, C., and Balter, V. (2015). Calcium isotopes reveal the trophic position of extant and fossil elasmobranchs. Chem. Geol. *415*, 118–125.

21. Elderfield, H., and Schultz, A. (1996). Mid-Ocean ridge hydrothermal fluxes and the chemical composition of the Ocean. Ann. Rev. Earth Planet. Sci. *24*, 191–224.

22. Heuser, A., Tütken, T., Gussone, N., and Galer, S.J.G. (2011). Calcium isotopes in fossil bones and teeth – Diagenetic versus biogenic origin. Geoch. Cosm. Acta. *75*, 3419–3433.

23. Reynard, B., and Balter, V. (2014). Trace elements and their isotopes in bones and teeth: diet, environments, diagenesis, and dating of archeological and paleontological samples. Palaeogeogr., Palaeoclim., Palaeoecol. *416*, 4–16.

24. Massare, J. (1987). Tooth morphology and prey preference of Mesozoic marine reptiles. J. Vertebr. Paleontol. *7*, 121–137.

25. Cury, P., and Shannon, L. (2004). Regime shift in upwelling ecosystems: observed changes and possible mechanisms in the northern and southern Benguela. Progr. Oceanogr. *60*, 223-243.

26. Lucas, J., and Prevot-Lucas, L. (1996). Tethyan phosphates and bioproductites. In Tethyan phosphates and bioproductites, A.E.M. Nairn et al., eds. (New York: Plenum Press), pp. 367–391.

27. Thierstein, H. R. (1982). Terminal Cretaceous plankton extinctions: a critical assessment. Geol. Soc. Am. Spec. Pap. *190*, 385–399.

28. Bernard, A., Lécuyer, C., Vincent, P., Amiot, R., Bardet, N., Buffetaut, E., Cuny, G., Fourel, F., Martineau, F., Mazin, J.-M. et al. (2010). Regulation of body temperature by some Mesozoic marine reptiles. Science *328*, 1379–1382.

29. Mourier, J., Maynard, J., Parravicini, V., Ballesta, L., Clua, E., Domeier, M.L., and Planes, S. (2016). Extreme inverted trophic pyramid of reef sharks supported by spawning groupers. Curr. Biol. *26*, 1–6.

30. Mitchell, J.S., Roopnarine, P.D., and Angielczyk, K.D. (2012). Late Cretaceous restructuring of terrestrial communities facilitated the end-Cretaceous mass extinction in North America. Proc. Nat. Acad. Sci. U.S.A. *109*, 18857–18861.

31. Tacail, T., Albalat, E., Telouk, P., and Balter, V. (2014). A simplified protocol for measurement of Ca isotopes in biological samples. J. Anal. Atom. Spectr. *29*, 529–535.

32. Tacail, T., Telouk, P., and Balter, V. (2015). Precise analysis of calcium stable isotope variations in biological apatites using laser ablation MC-ICPMS. J. Anal. Atom. Spectr. *31*, 152–162.

33. Bjorndal, K.A. (1980). Nutrition and grazing behaviour of the green turtle Chelonia mydas. Mar. Biol. *56*, 147–154.

34. Parker, D. M., Cooke, W. J., and Balazs, G. H. (2005). Diet of oceanic loggerhead sea turtles (*Caretta caretta*) in the central North Pacific. Fish. Bull. *103*, 142–152.

35. Farkaš, J., Buhl, D., Blenkinsop, J., and Veizer, J. (2007). Evolution of the oceanic calcium cycle during the late Mesozoic: evidence from $\delta^{44/40}$Ca of marine skeletal carbonates. Earth Planet. Sci. Lett. *253*, 96–111.

36. Farkaš, J., Böhm, F., Wallmann, K., Blenkinsop, J., Eisenhauer, A., Geldern, R., Munnecke, A., Voigt, S., and Veizer, J. (2007). Calcium isotope record of Phanerozoic oceans: implications for chemical evolution of seawater and its causative mechanisms. Geoch. Cosm. Acta *71*, 5117–5134.

37. Blättler, C.L., Henderson, G.M., and Jenkyns, H.C. (2012). Explaining the Phanerozoic Ca isotope history of seawater. Geology *40*, 843–846.

38. Soudry, D., Segal, I., Nathan, Y., Glenn, C.R., Halicz, L., Lewy, Z., and VonderHaa D.L. (2004). $^{44}Ca/^{42}Ca$ and $^{143}Nd/^{144}Nd$ isotope variations in Cretaceous-Eocene Tethyan francolites and their bearing on phosphogenesis in the southern Tethys. Geology *32*, 389–392.

39. Schmitt, A.D., Stille, P., and Vennemann T. (2003). Variations of the $^{44}Ca/^{40}Ca$ ratio in seawater during the past 24 million years: evidence from $\delta^{44}Ca$ and $\delta^{18}O$ values of Miocene phosphates. Geoch. Cosm. Acta *67*, 2607–2614.

40. Gussone, N., Böhm, F., Eisenhauer, A., Dietzel, M., Heuser, A., Teichert, B.M., and Dullo, W.C. (2005). Calcium isotope fractionation in calcite and aragonite. Geoch. Cosm. Acta *69*, 4485–4494.

STAR Methods

Contact for Reagent and Resource Sharing

Further information and requests for resources and reagents should be directed to and will be fulfilled by the Lead Contact, Jeremy Martin *(jeremy.martin@ens-lyon.fr)*.

Method Details

Sample collection

The total number of analyzed samples is 55 (Table S1). To the exception of 5 fossil marine turtle bones, all fossil vertebrate samples consist of tooth enamel obtained from 6 specimens belonging to 3 species of teleost fishes (n = 6), 9 specimens belonging to 3 species of large elasmobranchs (n = 9), 5 elasmosaurid teeth and 26 specimens belonging to 5 species of mosasaurids (n = 26).

In addition, modern turtle bone was also analysed (n = 4, see below). For marine turtles, chips of compact cortical bone were obtained from osteons. Cubes of fossil tooth enamel were sampled under a binocular using the tip of a scalpel. Dentine was easily discarded, as enamel would perfectly detach along the dentine-enamel junction. In two pycnodont teeth, which are rounded and highly resistant to mortar pressure, both enamel and dentine could not be separated. All samples come from a single locality and a single level (C2) of the Benguerir section, Ganntour Basin, Morocco, about 67 million year old.

Analytical methods

Chemical purification and analytical procedures follow what has been described in previous works [20, 31] using ion-exchange resins and purified acids (see Key Resources Table). The purified samples were measured on a Neptune Plus MC-ICP-MS at Laboratoire de Géologie de Lyon using the standard-sample bracketing method with ICP Ca Lyon as a standard [20, 31]. Isotopic compositions are expressed as delta values (in ‰) calculated using the $^{44}Ca/^{42}Ca$ ratio as follows:

$$\delta^{44/42}Ca = (((^{44}Ca/^{42}Ca)_{sample} / (^{44}Ca/^{42}Ca)_{ICP\ Ca\ Lyon}) - 1) \times 1000$$

All samples fall on a Ca mass fractionation line (Fig. S1). We report five independent measurements of NIST standard SRM 1486 (–1.00 ± 0.13 ‰, 2SD, n = 30; –1.06 ± 0.29 ‰, 2SD, n = 29; –1.00 ± 0.16 ‰, 2SD, n = 14; –1.03 ± 0.11 ‰, 2SD, n = 9; –1.02 ± 0.05 ‰, 2SD, n = 14) that are in good agreement with previously published values (–1.04 ± 0.11 ‰, 2SD[20]; –1.03 ± 0.13 ‰, 2SD [32]). Long-term reproducibility as measured for SRM 1486 is 0.12 ‰. All

values obtained in this study fall on a mass fractionation line with a slope of 0.507 (Fig. S1), in agreement with data from the literature [20]. The total range of measured values for $\delta^{44/42}$Ca in fossil remains from the Benguerir section, Morocco is 0.75‰ from –0.36‰ to –1.10‰ (Fig. 1 and Table S1). As in a previous study [20], taxonomic groups have overlapping values. The highest values of the dataset are part of the marine turtle group (median = – 0.37‰, n = 3) and of the teleost fishes (median = – 0.55‰, n = 6). The teleost group shows an outlier value (– 0.89‰) for a pycnodont tooth. $\delta^{44/42}$Ca values from large elasmobranch taxa are intermediate in the dataset (median = – 0.82‰, n = 6) with a single outlier, *Pristiphorus*, showing a high value similar to those of the marine turtle and teleost groups (– 0.52‰). The lowest values of the dataset were measured on marine reptile teeth (median = –0.96‰, n = 16).

Modern turtles

In order to have comparable datasets between environments of the modern world and that of the Cretaceous, a set of modern turtle samples was added to the modern selachian dataset [20]. Four specimens from the collections of Paléontologie of Université Claude Bernard Lyon 1 and representing three species of marine chelonioids were sampled and analysed for calcium isotopes. About half a milligram of skull bone was sampled on 1 specimen of *Caretta caretta* and 3 specimens of *Chelonia mydas*. *C. mydas* is a seagrass or algal grazer [33] and *C. caretta* feeds on invertebrates living on the surface [34]. The four turtle specimens analysed here have an average value of – 0.29 ± 0.03‰ (1SD, n = 4), which is slightly higher than the average value recovered for Maastrichtian marine turtles (– 0.40 ± 0.04‰ 1SD, n = 5). Implications for the reconstruction of the Maastrichtian seawater calcium isotope value are discussed below.

Seawater calcium evolution

The primary source of calcium in the marine environment is seawater but its calcium isotope composition has not been constant over the Phanerozoic due to changes in continental weathering regime and precipitation of carbonates by different types of marine biocalcifiers [35, 37]. In the modern world, the abundance of aragonitic calcifiers explains the relatively high calcium isotope ratio for seawater [36]. During the Cretaceous, calcitic calcifiers were dominant leading to an estimated difference of 0.05 – 0.07 ‰ toward lower isotope ratios for seawater. However, such small difference may not be measurable within the range of analytical error.

The calcium isotope value of seawater has been inferred for different time periods including the Jurassic and Cretaceous using fractionation factors between modern brachiopod calcite and seawater [35, 36]. However, for the Maastrichtian, no brachiopods have been analysed yet and the inference is based on the fractionation factor between authigenic marine phosphate [38] and seawater, which appears to be less well constrained than that inferred from brachiopod calcite values [35, 36] but yields a $\delta^{44/42}$Ca value of +0.26 ‰ for the lower Maastrichtian after conversion to ICP Ca Lyon has been applied.

Here, we calculate a fractionation factor between modern turtle bone (– 0.29 ± 0.03‰) and modern seawater (0.41‰ see Table 2 in[19]) using the equation presented in [35, 36]:

$$\alpha_{tb\text{-}sw} = (\delta^{44/42}Ca_{tb} + 1000) / (\delta^{44/42}Ca_{sw} + 1000) \quad (1)$$

where $\alpha_{tb\text{-}sw}$ corresponds to the fractionation factor between turtle bone (tb) and seawater (sw) and yields a value of 0.9993. Using $\alpha_{tb\text{-}sw}$ and the mean value for Maastrichtian turtle bone in this study (–0.40 ‰), we infer a calcium isotope value of +0.30 ‰ for seawater for the Late

Maastrichtian. This value is close, albeit lower by about 0.1‰ than the modern seawater value (+0.41‰). This value is comparable with the value inferred from seawater for the lower Maastrichtian using the francolite-seawater fractionation factor [39] (+0.26 ‰ converted to ICP Lyon [36]. Considering a biotic fractionation factor between modern brachiopods and seawater [35, 40], the lower Maastrichtian calcium isotope inferred value is +0.39‰, which is nearly identical to the $\delta^{44/42}$Ca value of seawater measured in the modern world.

Leaching experiments

Four fossil samples comprising two turtle bones and two mosasaur enamel samples (Fig. S2 and Table S1) were subjected to a test to assess the effect of diagenesis on the preservation of the original biogenic calcium isotopic composition. During mechanical sampling, the powder was split in half with one half for direct chemical purification and the other half for dilute acid etching. Acetic acid (0.1N) etching in an eppendorf tube takes 30 minutes after which the sample is rinsed three times with MQ water to remove potential $CaCO_3$ secondary precipitates. After this step, the leached sample undergoes chemical purification as any other samples treated in this study. The $\delta^{44/42}$Ca measurements of the leached versus untreated pairs show no detectable differences (Table S1 and Fig. S2).

Quantification and Statistical Analysis

Calcium isotope data discussed in the main text were analysed using non-parametric Wilcoxon-Mann Whitney tests. The errors discussed in the main text and featured in Figure 1, Figure S1, Figure S2 and Table S1 represent two standard deviations (2SD). The uncertainty displayed for

parameters of the linear model (origin and slope) in Figure S1 are the 95% confidence intervals (2 standard errors) and were calculated using the linear model function of the R software.

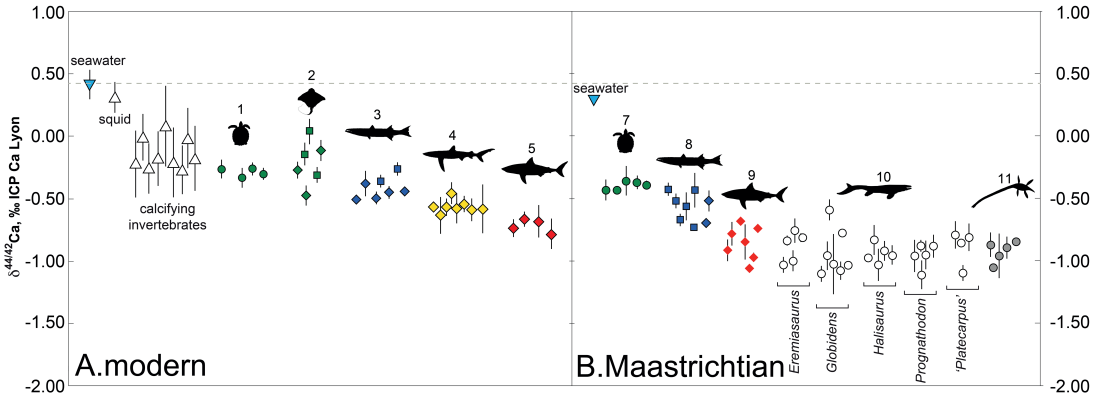

Figure 1. Modern versus Maastrichtian $\delta^{44/42}$Ca (in ‰ relative to ICP Ca Lyon standard) variability in marine ecosystems of the modern world (A) and of the Maastrichtian (B). For the modern dataset, data compilation is from the literature (see [19] for details) to the exception of modern marine turtles (this study). The fossil dataset is entirely new to this study. 1, modern marine turtles; 2, zooplanktivores; 3, primary piscivores; 4, secondary piscivores; 5, tertiary piscivores; 7, Maastrichtian marine turtles; 8, Maastrichtian primary piscivores; 9, Maastrichtian teriary piscivores; 10, mosasaurs; 11, plesiosaurs. Squares indicate teleost fishes and diamonds indicate elasmobranchs. Error bars represent 2SD. Triangles represent invertebrates; circles represent marine reptiles; squares represent teleost fishes; diamonds represent elasmobranchs. See also Table S1.

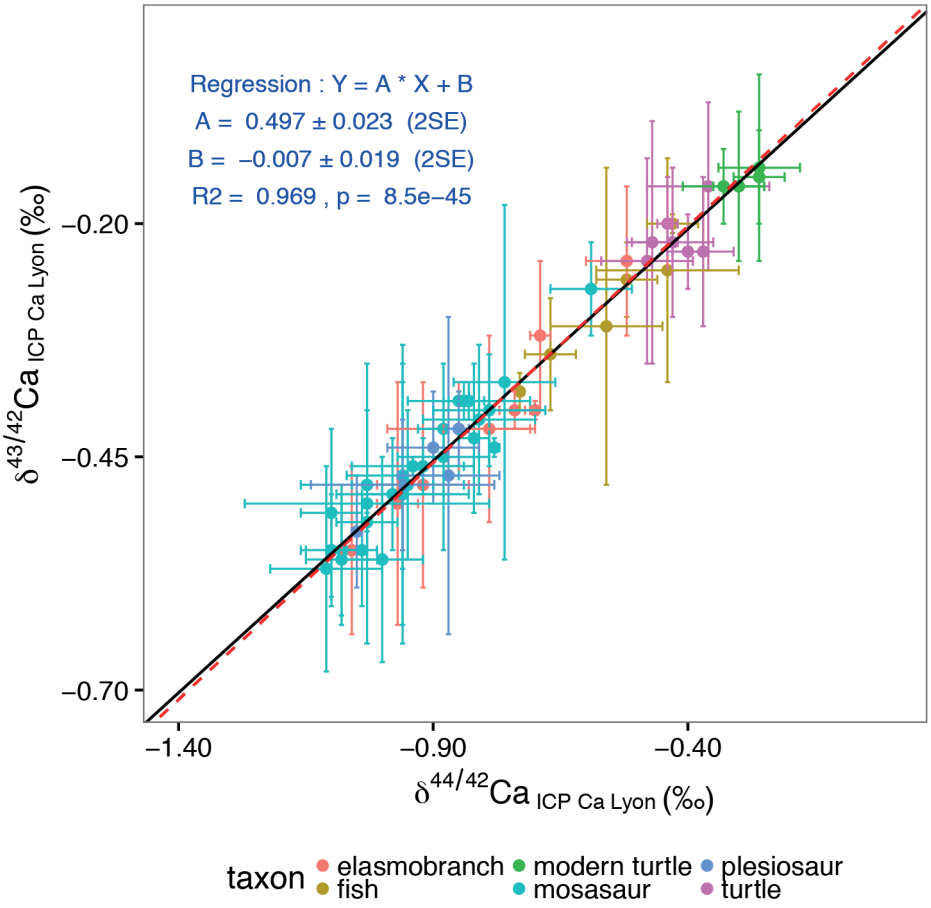

Figure S1. Triple isotope plot of all the data analysed in this study. All datapoints fall on a mass fractionation line (black line) in agreement with the 0.507 slope predicted by exponential mass fractionation law (indicated with the dashed red line). **Related to STAR Methods.**

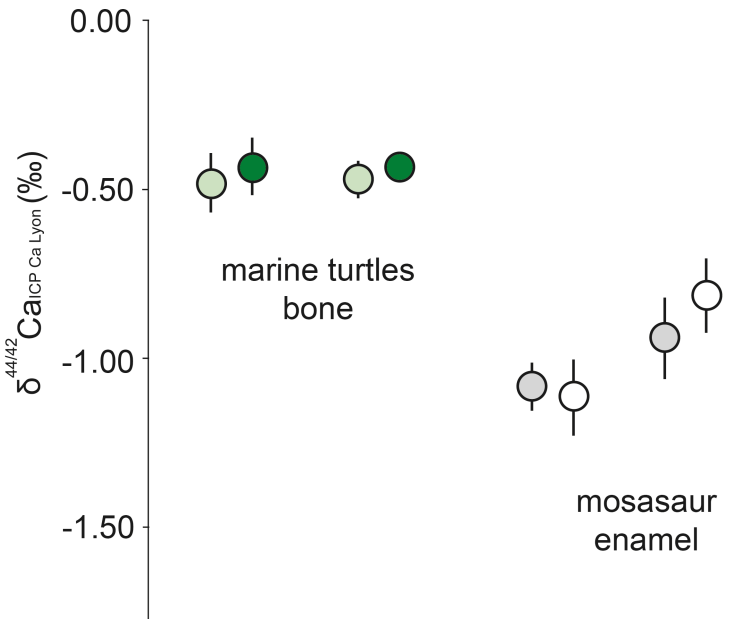

Figure S2. $\delta^{44/42}$Ca values measured in this study for treated and untreated fossil samples. Comparison of $\delta^{44/42}$Ca values measured on pairs of treated (to the left) versus untreated (to the right) samples (in ‰ relative to ICP Ca Lyon standard). Error bars represent 2SD. **Related to START Methods and Table S1.**

curation n°	age	consumer level	lab name	material	higher taxonomy	taxon	δ44/42Ca (‰)	2SD	δ43/42Ca (‰)	2SD	n
OCP-SA 1500	Maastrichtian	zooplanktivore	Ma-T1	bone	marine turtle	Bothremydidae indet.	-0.36	0.12	-0.16	0.09	4
OCP-SA 1501	Maastrichtian	zooplanktivore	Ma-T2	bone	marine turtle	Bothremydidae indet.	-0.40	0.04	-0.23	0.04	4
OCP-SA 1502	Maastrichtian	zooplanktivore	Ma-T3	bone	marine turtle	Chelonioidea indet.	-0.37	0.06	-0.23	0.08	5
OCP-SA 1503	Maastrichtian	zooplanktivore	Ma-T4	bone	marine turtle	indet.	-0.44	0.02	-0.20	0.05	3
OCP-SA 1504	Maastrichtian	zooplanktivore	Ma-T5	bone	marine turtle	indet.	-0.43	0.08	-0.22	0.08	3
OCP-SA 1505	Maastrichtian	primary	Ma-En1	tooth enamel	teleost fish	*Enchodus* sp. A	-0.43	0.05	-0.20	0.01	3
OCP-SA 1506	Maastrichtian	primary	Ma-En2	tooth enamel	teleost fish	*Enchodus* sp. A	-0.52	0.06	-0.26	0.04	3
OCP-SA 1507	Maastrichtian	primary	Ma-Enli1	tooth enamel	teleost fish	*Enchodus* sp. B	-0.67	0.05	-0.34	0.06	3
OCP-SA 1508	Maastrichtian	primary	Ma-Enli2	tooth enamel	teleost fish	*Enchodus* sp. B	-0.56	0.11	-0.31	0.17	3
OCP-SA 1509	Maastrichtian	primary	Ma-Py1	tooth enamel	teleost fish	Pycnodont	-0.73	0.00	-0.38	0.02	3
OCP-SA 1510	Maastrichtian	primary	Ma-Py2	tooth enamel	teleost fish	Pycnodont	-0.44	0.14	-0.25	0.12	3
OCP-SA 1511	Maastrichtian	primary	Ma-Pri1	tooth enamel	elasmobranch	*Pristiphorus* sp.	-0.70	0.02	-0.40	0.01	2
OCP-SA 1512	Maastrichtian	primary	Ma-Pri2	tooth enamel	elasmobranch	*Pristiphorus* sp.	-0.52	0.08	-0.24	0.08	3
OCP-SA 1513	Maastrichtian	tertiary	Ma-Cr1	tooth enamel	elasmobranch	*Cretolamna* sp.	-0.92	0.09	-0.48	0.11	3
OCP-SA 1514	Maastrichtian	tertiary	Ma-Cr2	tooth enamel	elasmobranch	*Cretolamna* sp.	-0.79	0.09	-0.42	0.10	4
OCP-SA 1515	Maastrichtian	tertiary	Ma-sq1	tooth enamel	elasmobranch	*Squalicorax* sp.	-0.69	0.02	-0.32	0.08	3
OCP-SA 1516	Maastrichtian	tertiary	Ma-sq2	tooth enamel	elasmobranch	*Squalicorax* sp.	-0.85	0.14	-0.42	0.05	3
OCP-SA 1517	Maastrichtian	tertiary	Car1	tooth enamel	elasmobranch	*Carcharias* sp.	-1.06	0.02	-0.55	0.09	2
OCP-SA 1518	Maastrichtian	tertiary	Car2	tooth enamel	elasmobranch	*Carcharias* sp.	-0.97	0.04	-0.50	0.13	2
OCP-SA 1519	Maastrichtian	tertiary	Car3	tooth enamel	elasmobranch	*Carcharias* sp.	-0.74	0.03	-0.40	0.02	2
OCP-SA 1520	Maastrichtian	tertiary	Ma-Ere1	tooth enamel	mosasaurid	*Eremiasaurus* sp.	-1.03	0.06	-0.52	0.01	3
OCP-SA 1521	Maastrichtian	tertiary	Ma-Ere2	tooth enamel	mosasaurid	*Eremiasaurus* sp.	-1.00	0.08	-0.56	0.11	3
OCP-SA 1522	Maastrichtian	tertiary	Ma-Ere3	tooth enamel	mosasaurid	*Eremiasaurus* sp.	-0.84	0.04	-0.39	0.02	3
OCP-SA 1523	Maastrichtian	tertiary	Ma-Ere4	tooth enamel	mosasaurid	*Eremiasaurus* sp.	-0.76	0.10	-0.37	0.19	2
OCP-SA 1524	Maastrichtian	tertiary	Ma-Ere5	tooth enamel	mosasaurid	*Eremiasaurus* sp.	-0.82	0.03	-0.43	0.08	3
OCP-SA 1525	Maastrichtian	tertiary	Ma-G1	tooth enamel	mosasaurid	*Globidens* sp.	-0.78	0.01	-0.44	0.01	3
OCP-SA 1526	Maastrichtian	tertiary	Ma-G2	tooth enamel	mosasaurid	*Globidens* sp.	-0.59	0.08	-0.27	0.05	3
OCP-SA 1527	Maastrichtian	tertiary	Ma-G4	tooth enamel	mosasaurid	*Globidens* sp.	-1.03	0.24	-0.50	0.15	3
OCP-SA 1528	Maastrichtian	tertiary	Ma-G3	tooth enamel	mosasaurid	*Globidens* sp.	-0.96	0.11	-0.47	0.10	3
OCP-SA 1529	Maastrichtian	tertiary	Ma-G5	tooth enamel	mosasaurid	*Globidens* sp.	-1.10	0.06	-0.55	0.06	3
OCP-SA 1530	Maastrichtian	tertiary	Ma-G6	tooth enamel	mosasaurid	*Globidens* sp.	-1.04	0.03	-0.55	0.06	4
OCP-SA 1531	Maastrichtian	tertiary	Ma-G7	tooth enamel	mosasaurid	*Globidens* sp.	-1.08	0.07	-0.55	0.07	2
OCP-SA 1532	Maastrichtian	tertiary	Ma-H3	tooth enamel	mosasaurid	*Halisaurus* sp.	-0.98	0.02	-0.49	0.06	3
OCP-SA 1533	Maastrichtian	tertiary	Ma-H4	tooth enamel	mosasaurid	*Halisaurus* sp.	-0.83	0.12	-0.39	0.02	2
OCP-SA 1534	Maastrichtian	tertiary	Ma-H5	tooth enamel	mosasaurid	*Halisaurus* sp.	-1.03	0.13	-0.48	0.08	2
OCP-SA 1535	Maastrichtian	tertiary	Ma-H1	tooth enamel	mosasaurid	*Halisaurus* sp.	-0.92	0.08	-0.46	0.03	3
OCP-SA 1536	Maastrichtian	tertiary	Ma-H2	tooth enamel	mosasaurid	*Halisaurus* sp.	-0.96	0.08	-0.49	0.14	3
OCP-SA 1537	Maastrichtian	tertiary	Ma-Pro1	tooth enamel	mosasaurid	*Prognathodon* sp.	-0.96	0.13	-0.49	0.16	4
OCP-SA 1538	Maastrichtian	tertiary	Ma-Pro2	tooth enamel	mosasaurid	*Prognathodon* sp.	-1.11	0.11	-0.57	0.11	3
OCP-SA 1539	Maastrichtian	tertiary	Ma-Pro3	tooth enamel	mosasaurid	*Prognathodon* sp.	-0.95	0.11	-0.48	0.08	2
OCP-SA 1540	Maastrichtian	tertiary	Ma-Pro4	tooth enamel	mosasaurid	*Prognathodon* sp.	-0.88	0.09	-0.45	0.10	3
OCP-SA 1541	Maastrichtian	tertiary	Ma-Pro5	tooth enamel	mosasaurid	*Prognathodon* sp.	-0.88	0.05	-0.42	0.02	2
OCP-SA 1542	Maastrichtian	tertiary	Ma-Pus1	tooth enamel	mosasaurid	"*Platecarpus*" *ptychodon*	-1.10	0.06	-0.51	0.09	3
OCP-SA 1543	Maastrichtian	tertiary	Ma-Pus2	tooth enamel	mosasaurid	"*Platecarpus*" *ptychodon*	-0.81	0.11	-0.41	0.08	4
OCP-SA 1544	Maastrichtian	tertiary	Ma-Pus3	tooth enamel	mosasaurid	"*Platecarpus*" *ptychodon*	-0.79	0.11	-0.40	0.06	2
OCP-SA 1545	Maastrichtian	tertiary	Ma-Pus4	tooth enamel	mosasaurid	"*Platecarpus*" *ptychodon*	-0.85	0.02	-0.39	0.00	2
OCP-SA 1546	Maastrichtian	tertiary	Ma-P1	tooth enamel	elasmosaurid	indet.	-0.85	0.02	-0.42	0.04	3
OCP-SA 1547	Maastrichtian	tertiary	Ma-P2	tooth enamel	elasmosaurid	indet.	-0.87	0.10	-0.47	0.17	3
OCP-SA 1548	Maastrichtian	tertiary	Ma-P3	tooth enamel	elasmosaurid	indet.	-1.05	0.01	-0.53	0.06	3
OCP-SA 1549	Maastrichtian	tertiary	Ma-P5	tooth enamel	elasmosaurid	indet.	-0.96	0.18	-0.48	0.07	3
OCP-SA 1550	Maastrichtian	tertiary	Ma-P4	tooth enamel	elasmosaurid	indet.	-0.90	0.09	-0.44	0.06	3
OCP-SA 1538	Maastrichtian	tertiary	Ma-Pro2lea	tooth enamel	mosasaurid	*Prognathodon* sp. leached	-1.08	0.07	-0.56	0.07	4
OCP-SA 1543	Maastrichtian	tertiary	Ma-Pus2lea	tooth enamel	mosasaurid	*P. ptychodon* leached	-0.94	0.12	-0.46	0.01	*2*
OCP-SA 1503	Maastrichtian	zooplanktivore	Ma-T4lea	bone	marine turtle	indet.	-0.47	0.05	-0.22	0.13	3
OCP-SA 1504	Maastrichtian	zooplanktivore	Ma-T5lea	bone	marine turtle	indet.	-0.48	0.09	-0.24	0.11	3
UCBL-FSL-94808	modern	zooplanktivore	Chel1	bone	marine turtle	*Caretta caretta*	-0.26	0.08	-0.14	0.10	*4*
UCBL-FSL-532088	modern	zooplanktivore	Chel3	bone	marine turtle	*Chelonia mydas*	-0.33	0.08	-0.16	0.04	*4*
UCBL-FSL-532403	modern	zooplanktivore	Chel4	bone	marine turtle	*Chelonia mydas*	-0.26	0.05	-0.15	0.05	*4*
UCBL-FSL-532095	modern	zooplanktivore	Chel5	bone	marine turtle	*Chelonia mydas*	-0.30	0.05	-0.16	0.08	*3*

Table 1. Calcium isotope values (expressed as δ44/42Ca (in ‰) relative to standard ICP Ca-Lyon) measured in this study for marine vertebrates of the Maastrichtian of Morocco as well as for modern marine turtle bone. Institutional abbreviations: OCP-SA, Office Chérifien des Phosphates, Khouribga, Morocco; UCBL-FSL, Université Claude Bernard Lyon 1, Faculté des Sciences de Lyon, Villeurbanne, France. **Related to STAR Methods.**